Three-state Potts model on the centered triangular lattice

Fu, Z.; Guo, W.N.; Blöte, H.W.J.

Three-state Potts model on the centered triangular lattice

Zhe Fu
College of Physics and Electronic Engineering, Xinxiang University, Xinxiang 453003, China

Wenan Guo*
Physics Department, Beijing Normal University, Beijing 100875, China
and Beijing Computational Science Research Center, Beijing 100193, China

Henk W. J. Blöte†
Instituut Lorentz, Leiden University, P.O. Box 9506, 2300 RA Leiden, the Netherlands

(Received 18 September 2019; published 14 January 2020)

We study phase transitions of the Potts model on the centered-triangular lattice with two types of couplings, namely, K between neighboring triangular sites, and J between the centered and the triangular sites. Results are obtained by means of a finite-size analysis based on numerical transfer-matrix calculations and Monte Carlo simulations. Our investigation covers the whole (K, J) phase diagram, but we find that most of the interesting physics applies to the antiferromagnetic case $K < 0$, where the model is geometrically frustrated. In particular, we find that there are, for all finite J, two transitions when K is varied. Their critical properties are explored. In the limits $J \to \pm\infty$ we find algebraic phases with infinite-order transitions to the ferromagnetic phase.

DOI: 10.1103/PhysRevE.101.012118

I. INTRODUCTION

The Potts model [1] is defined in terms of q-state lattice variables, also called spins, $\sigma_i = 1, 2, \ldots, q$, where i stands for the lattice site of the variable. Neighboring spins interact only if they are equal. Since its introduction, the model has played a significant role in statistical physics [2,3] and in applications to various condensed-matter systems [4].

Originally, most studies of the Potts model focused on ferromagnetic interactions, and for that case the critical properties and phase diagram are well known. However, more recently the antiferromagnetic(AF) Potts model also has received considerable attention, because of its rich and lattice-dependent behavior. For instance, the behavior of the AF $q = 3$ Potts model on several lattices appears to be quite different. The model displays a weak first-order transition at a nonzero temperature on the triangular lattice [5], an ordinary finite-temperature critical point on the diced lattice [6], and on the honeycomb lattice it is disordered at all non-negative temperatures [7]. On the square lattice, it is critical at zero temperature and disordered at positive temperatures [8–11]. On a set of planar lattices called quadrangulations the model either has a zero-temperature critical point, or it has three ordered coexisting phases, dependent on whether or not the quadrangulation is self-dual [12]. In view of this lattice-dependent behavior, AF Potts models have to be investigated case by case.

From another point of view, AF Potts models on many regular lattices have an interesting feature: there exists a lattice-dependent critical value q_c of q beyond which there is no transition. The generalization of the Potts model to the random-cluster model [13], in which q is a continuous variable, enables the determination of q_c even if it is not an integer. For example, $q_c = \frac{1}{2}(3 + \sqrt{5})$ for the honeycomb lattice was determined [14] by examining the known critical frontiers in the light of AF interactions. However, Huang *et al* [15] have discovered a set of lattices on which the AF Potts model does not have such a q_c. Furthermore, some AF Potts models on irregular lattices, in which the number of sites is different for different sublattices, display entropy-driven transitions at a finite temperature to partially ordered phases at a value of q larger than the q_c that one would naively expect [6,15–18].

The present work considers the case of the $q = 3$ model on the centered triangular lattice, also known as the Asanoha or hemp-leaf lattice [19], which is sketched in Fig. 1. The interactions are specified by the reduced Hamiltonian

$$H/k_BT = -K \sum_{\langle i,j \rangle} \delta_{\sigma_i \sigma_j} - J \sum_{[k,l]} \delta_{\sigma_k \sigma_l}, \tag{1}$$

where the sum on $\langle i, j \rangle$ runs over all bonds connecting nearest-neighbor spins on the triangular sites, and the sum on $[k, l]$ runs over all bonds between the centered spins and their three triangular neighbor spins. The corresponding Potts couplings are denoted by K and J. In the case $J = 0$ the model reduces to the $q = 3$ Potts model on the triangular lattice. For $K = 0$ the model reduces to the $q = 3$ Potts model on the diced lattice.

II. ALGORITHMS AND TESTS

A transfer-matrix algorithm using the $q = 3$ spin representation was employed for the calculation of the free energy

*waguo@bnu.edu.cn
†henk@lorentz.leidenuniv.nl

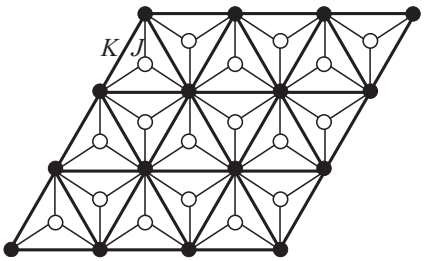

FIG. 1. The centered triangular lattice. The triangular vertices (•) as well as the centered vertices (○) are occupied by three-state Potts spins. Neighboring spins on the triangular sites are coupled with strength K, and the centered sites are coupled with strength J to their triangular neighbors.

densities and magnetic correlation lengths for finite sizes up to $L = 18$. The spin systems studied were wrapped on $L \times \infty$ cylinders, with periodic boundary conditions in the finite direction, using a length unit equal to the triangular edges. The transfer-matrix algorithm is applicable for all J and K. It does, in most cases, allow rather accurate determinations of phase transitions and some universal parameters. In those cases where we did not require very precise results, for instance, for the global determination of phase boundaries, we also applied a Metropolis-type Monte Carlo algorithm.

A. Miscellaneous results of the transfer-matrix algorithm

In the case $J = 0$ the model reduces to the $q = 3$ Potts model on the triangular lattice. We first consider the ferromagnetic case $K > 0$ and required that the magnetic correlation lengths $\xi(K, L)$ satisfies Cardy's asymptotic relation [20] $L/\xi(K, L) \simeq 2\pi X_h$, where $X_h = 2/15$ is the exactly known [21] magnetic dimension. We solved K for each value of $2 < L \leqslant 18$, and we thus obtained a series of estimates of the critical point. Extrapolation by finite-size scaling [22], using correction exponents $y_{\rm irr} - y_t = -2$ [21] and -4, led to a best estimate $K_{\rm c,triangular} = 0.630944725(5)$. This value is close to the exactly known critical point $\ln[2\cos(\pi/9)]$ [4,23], thus providing a consistency check. For $K = 0$ the model reduces to the $q = 3$ Potts model on the diced lattice. A similar analysis yielded finite-size estimates of its ferromagnetic critical point $J_{\rm c,diced}$ in the range $2 < L \leqslant 18$. Extrapolation led to a best estimate $J_{\rm c,diced} = 0.955032665(5)$. This value is close to an unpublished transfer-matrix result $J_{\rm c,diced} = 0.9550325(23)$ as quoted by Wu and Guo [14]. Our result for the diced lattice also yields, by duality, the critical coupling of the $q = 3$ Potts model on the kagome lattice as $K_{\rm c,kagome} = 1.056560222(5)$. This is in agreement with 1.05656027(7) as obtained by Jacobsen and Scullard [24], and 1.0565602231(1) as obtained by Jacobsen [25]. Furthermore we performed a similar analysis for the antiferromagnetic $q = 3$ Potts model on the diced lattice, from which we estimate $J_{\rm c,diced\,AF} = -1.9703946(5)$.

III. PHASE DIAGRAM IN THE (K, J) PLANE

One can distinguish three different regions, according to the relative magnitudes of the weights W_{111} of a triangle with three equal spins, W_{112} for only two equal spins, and W_{123} for three different spins. Since each K coupling is shared between two triangles, only one half of it is included in these weights. Furthermore the centered spins are summed out, so that the weights depend only on the triangular spins, while they still include the effect of J:

$$W_{111} = \exp(3K/2 + 3J) + 2\exp(3K/2),$$
$$W_{112} = \exp(K/2 + 2J) + \exp(K/2 + J) + \exp(K/2),$$
$$W_{123} = 3\exp(J).$$

For $J \gg 0$ we have $\ln W_{111} \simeq 3K/2 + 3J$. For $J \ll 0$ the centered spins will assume a state different from their triangular neighbors, so that $\ln W_{111} \simeq 3K/2$. For K sufficiently large negative, the weight W_{123} will dominate, and frustration of the centered spins will lead to $\ln W_{123} \simeq J$. One also expects an intermediate region dominated by triangles having two equal spins, with $\ln W_{112} \simeq K/2 + 2J$ for $J \gg 0$ and $K/2$ for $J \ll 0$.

The phase boundaries are approximately located where the weights of two neighboring phases become equal. Thus we expect the following phases, shown in Fig. 2(a):

(1) The ferromagnetic region, dominated by the weight W_{111}. For $J > 0$ it is located at $K \gtrsim -J$, and for $J < 0$ at $K \gtrsim 0$.

(2) The intermediate region, dominated by the weight W_{112}. For $J > 0$ it is located at $-2J \lesssim K \lesssim -J$, and for $J < 0$ at $2J \lesssim K \lesssim 0$.

(3) The antiferromagnetic region, dominated by the weight W_{123}. For both signs of J it is located at $K \lesssim -2|J|$.

Monte Carlo, exact, and transfer-matrix results, shown in Fig. 2(b), confirm this expectation. It appears that the intermediate phase is disordered, at least as long as $|J|$ is not too large. Partial order appears for large $|J|$, whose nature will be explored in the following subsections.

Ferromagnetic $q = 3$ universality applies naturally to the transition line between regions 1 and 2. As for the antiferromagnetic transition line, the triangular model at $J = 0$ was found to undergo a weak first-order transition; see, for instance, Adler *et al.* [5] and references therein. This transition is located near $K = -1.594482(8)$ [26].

A. Mapping on the honeycomb O(2) loop model

In the special case of the limits

$$|J| \to \infty, \quad K \gg -2|J|, \tag{2}$$

the spin model becomes equivalent with the nonintersecting O(2) loop model on the honeycomb lattice. That model displays a range where the magnetic correlation function decays algebraically [27]. This proves that the spin model must reach a critical state at the corresponding parameters.

The construction of an O(2) loop configuration from an allowed $q = 3$ Potts spin configuration is formulated as follows. We first note that elementary triangles with three different spins on the triangular vertices would cost an energy $\propto |J|$ and are therefore excluded. Each allowed triangle contains precisely one or three edges connecting equal spins. This is illustrated in Fig. 3 by erasing all triangular edges connecting unequal spins, leading to a graph with one or three edges remaining about each elementary triangular face. Next, construct a dual graph from edges connecting each pair of dual sites if not separated by a remaining triangular edge. Thus,

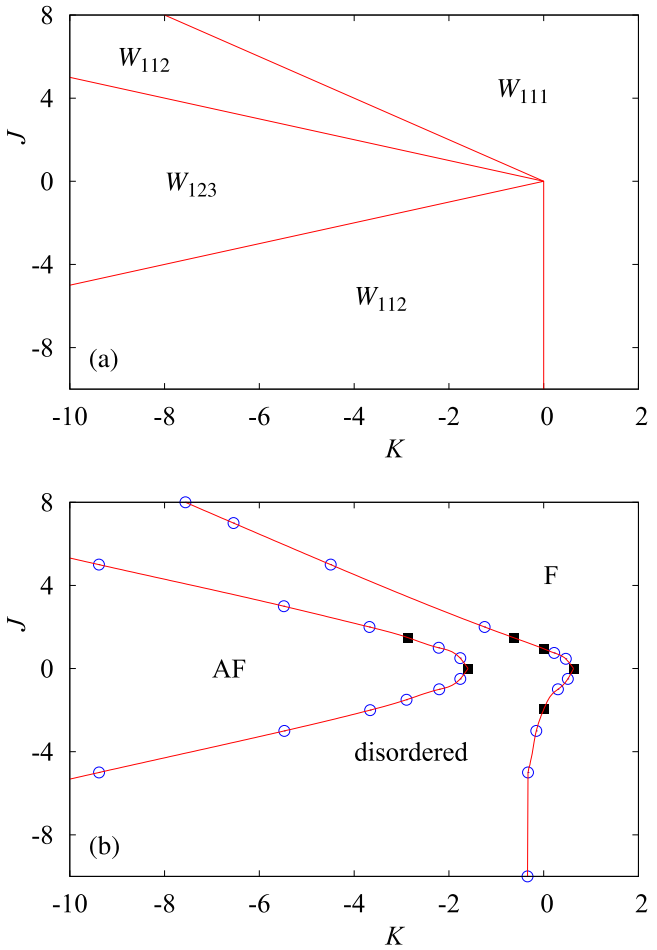

FIG. 2. Phase diagram of the centered triangular $q = 3$ Potts model. (a) The division of the (K, J) diagram according to the dominance of the leading terms in the weights W_{111}, W_{112}, and W_{123} described in the text. (b) The numerical results for the phase boundaries, obtained by Monte Carlo simulations, except those shown as black squares (■), which are accurate results obtained by other methods, as mentioned in the text, and by application of the star-triangle transformation to the two $J = 0$ points. For all finite J, one observes three different phases: an antiferromagnetic (AF) one, an intermediate (disordered) one, and a ferromagnetic (F) one.

each dual site connects to zero or two edges on the dual honeycomb lattice. In this way one obtains a configuration of closed loops on the honeycomb lattice. Thus the triangular neighbor spins are equal if and only if they are not separated by such a loop. The introduction of a new loop in a region of triangular Potts spins equal to $\sigma_{\rm old}$ will thus change the inside spin configuration. The spin degrees of freedom allow the centered spins on the loop to take two values

$$\tau = \sigma_{\rm old} \pm 1 \mod 3 \tag{3}$$

(with the convention $1 \leqslant k \mod 3 \leqslant 3$), while $\sigma_{\rm old}$ remains the value of the triangular spins directly outside the loop. Then each triangular spin along the inside perimeter of the loop must change its old value $\sigma_{\rm old}$ in

$$\sigma_{\rm new} = \sigma_{\rm old} \mp 1 \mod 3, \tag{4}$$

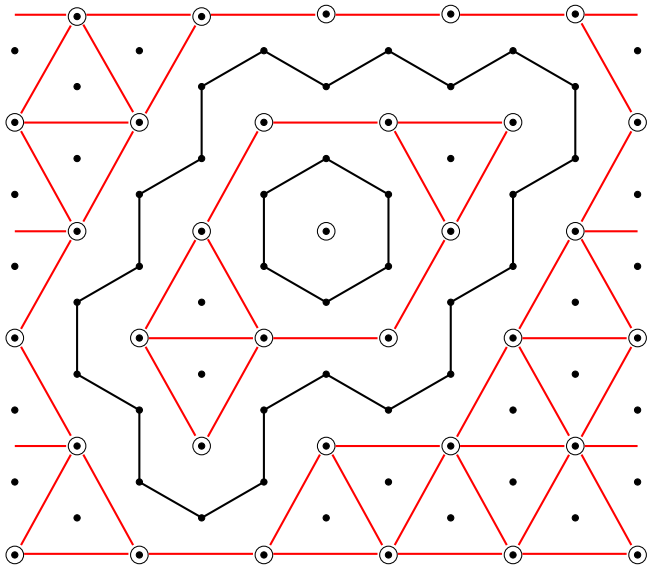

FIG. 3. Equivalence of the centered triangular model with the O(n) loop model on the honeycomb lattice, under the condition that triangles with three different Potts spins are excluded. This condition applies in the limits $J \to \pm\infty$ when $K \gg -2|J|$. Triangular edges between equal Potts spins are shown in red. The honeycomb loops separate unequal triangular spins. Centered spins connected by a black loop segment are equal.

so that these inside spins are unequal to the spins on the loop, and unequal to the outside spins. Application of this rule (4) to *all* spins inside the new loop guarantees that the energy changes are restricted to the bonds crossing that loop, even if the region inside the loop contains further loops. The spin degeneracy expressed in Eqs. (3) and (4) translates into a weight factor 2 for each loop on the honeycomb lattice.

To complete the mapping onto the O(n) model, we still have to obtain the weight x of each loop segment. This is done by comparing the weight of a loop to the weight ratio of spin configurations with and without a loop. In the O(n) model, the weight of a loop consisting of $n_{\rm s}$ loop segments is $w_{\rm loop} = nx^{n_{\rm s}}$, while the vacuum has weight $w_{\rm vac} = 1$. The loop intersects $n_{\rm s}$ triangles with weight W_{112}. Removal of this loop changes their weight into W_{111}. Thus the weight of the loop is $2[W_{112}/W_{111}]^{n_{\rm s}}$ in the spin language. The expression for the weight ratio depends on the sign of J.

(1) In the case $J \to -\infty$ the terms in W_{111} and W_{112} that contain J vanish, and $W_{112}/W_{111} = \exp(-K)/2$.

(2) For $J \to +\infty$ the terms in W_{111} and W_{112} with the largest prefactors of J survive, and $W_{112}/W_{111} = \exp(-K - J)$.

A comparison of the weights of the configurations with and without a loop in both representations directly determines the O(n) loop weight n and the relation between x and the Potts couplings:

$$w_{\rm loop}/w_{\rm no\,loop} = nx^{n_{\rm s}} = 2[\exp(-K)/2]^{n_{\rm s}} \text{ for } J \to -\infty, \tag{5}$$

$$w_{\rm loop}/w_{\rm no\,loop} = nx^{n_{\rm s}} = 2[\exp(-K - J)]^{n_{\rm s}} \text{ for } J \to +\infty. \tag{6}$$

The partition sum of the loop model is defined as

$$Z_{\rm loop}(x,n)=\sum_{\mathcal{G}} x^{n_{\rm b}} n^{n_{\rm l}}, \tag{7}$$

where the sum is on all loop configurations $\mathcal{G}$, $n_{\rm b}$ is the number of honeycomb edges covered by $\mathcal{G}$, and $n_{\rm l}$ is the number of loops. The prefactor in its relation with the partition sum $Z_{\rm ctri}$ of the spin model can, for instance, be found from a comparison between the Boltzmann factors of the loop vacuum in the two representations. The resulting relation between the two models is summarized as

$$Z_{\rm ctri}(K,J)=2^{2N}e^{3NK}Z_{\rm loop}(x,n),$$
$$n=2,\quad x=e^{-K}/2\quad \text{for } J\to-\infty, \tag{8}$$

$$Z_{\rm ctri}(K,J)=e^{3N(K+2J)}Z_{\rm loop}(x,n),$$
$$n=2,\quad x=e^{-K-J}\quad \text{for } J\to+\infty, \tag{9}$$

where N is the number of triangular sites. The free energies, per the triangular and honeycomb site, respectively, are thus related as $f_{\rm ctri}(K)=2\ln 2+3K+2f_{\rm loop}(x,n)$ for $J\to-\infty$ and as $f_{\rm ctri}(K)=3K+6J+2f_{\rm loop}(x,n)$ for $J\to+\infty$.

B. The fully packed loop model

For $K\to-\infty$, but still subject to Eq. (2), the weight of the honeycomb edges not covered by a loop vanishes, and we obtain the fully packed O(2) model. This model displays a rather special behavior [28,29]; for instance, its conformal anomaly was found to be equal to 2. This value can be interpreted in terms of two SOS-like degrees of freedom, one of which comes from the O(2) model, and the other from the equivalence [28] of the fully packed loop model with the triangular SOS model [30]. Using the O(2) loop representation, we have extended the transfer-matrix calculations of the free energy up to finite size $L=21$. The conformal anomaly can be estimated for each single system size that is a multiple of 3, using the free energy per honeycomb site for the infinite system, which is known from an exact result by Baxter [31] as

$$\lim_{x\to\infty} f_{\rm loop}(x)-x=\frac{1}{2}\ln\prod_{i=1}^{\infty}\frac{(3i-1)^2}{3i(3i-2)}, \tag{10}$$

which can be approximated as $\lim_{x\to\infty} f_{\rm loop}-x=0.189560048316\ldots$. Taking into account the geometric factor $\zeta=2/\sqrt{3}$, which is needed to obtain the free energy density of the honeycomb lattice instead of the free energy per site, the finite-size estimates are [32,33]

$$c_{\rm est}(x,L)=4\sqrt{3}L^2[f_{\rm loop}(x,L)-f_{\rm loop}(x,\infty)]/\pi. \tag{11}$$

The usual extrapolation of these estimates by power-law fits, assuming power-law corrections as L^{-2}, yields iterated estimates of $c(\infty)$ close to 2, with differences of a few times 10^{-2}, suggesting the presence of a logarithmic correction. Including an extrapolation step as $c_{\rm est}(x\to\infty,L)\simeq c(x\to\infty)[1+\frac{a}{L^2(b+\ln L)}]$ led to a better apparent convergence, with the last two iteration steps within 10^{-4} from $c=2$.

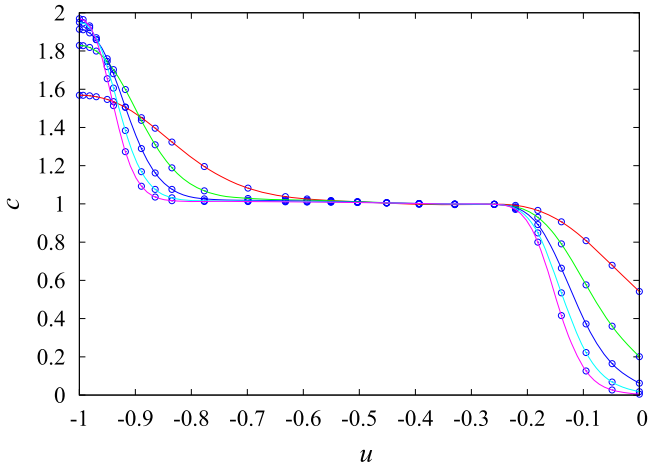

FIG. 4. Finite-size estimates of the conformal anomaly c as a function of $u=e^K-1$ of the $J\to-\infty$ centered triangular $q=3$ antiferromagnetic Potts model. Estimates for system sizes L that are multiples of 3 are obtained by solving for c in Eq. (11), from the free energies for systems with sizes L and $L-3$. Results are shown for $L=6$, 9, 12, 15, and 18. Larger system sizes correspond with steeper curves. This behavior applies as well in the limit $J\to+\infty$ after redefining $u=e^{K+J}-1$. These results still depend on the absence of type (1,2,3) triangles, implying $K/|J|>-2$.

C. Phase changes induced by K

For finite values of $|K|$, but still subject to condition (2), the model is still exactly equivalent with the O(2) loop model but no longer fully packed. The fugacity of empty honeycomb vertices is relevant [28], and crossover takes place to the universal behavior of the dense phase of the O(2) model which has $c=1$. This crossover is illustrated by the finite-size estimates of the conformal anomaly in Fig. 4. This figure uses the parametrization $u=e^K-1$ so that the whole antiferromagnetic range $K<0$ can be included.

When $|K|$ is sufficiently lowered, the spin model undergoes an infinite-order Berezinskii-Kosterlitz-Thouless transition [34] to a state with ferromagnetic order on the triangular sites, and disordered spins on the honeycomb sites. The transition to the $c=0$ phase (loops diluted, and ferromagnetic in the language of the spins on the triangular lattice) is visible in the right-hand side of Fig. 4 and was numerically located from the requirement

$$X_h(K,L)\equiv L/[2\pi\xi(K,L)]=2/9, \tag{12}$$

where 2/9 is the expected value of the magnetic dimension of the transition; see, for instance, the similar analysis in Ref. [35]. We thus estimate $K_{\rm BKT}=-0.3465(1)$, in good agreement with the exact value $-\ln(2)/2$, which follows from Eq. (8) and $x_{\rm c}=1/\sqrt{2}$ [27].

The mapping on the O(n) model relies on the condition (2). Next, we drop the condition that limits K in Eq. (2), while maintaining the limit $|J|\to\infty$. Then type (1,2,3) triangles are no longer excluded, and the mapping on the O(n) model is no longer valid. One expects a transition near $K\approx 2J$ to the antiferromagnetic phase. We investigated this point using transfer-matrix calculations, based on finite-size scaling of the magnetic correlation length. The behavior of the scaled gaps,

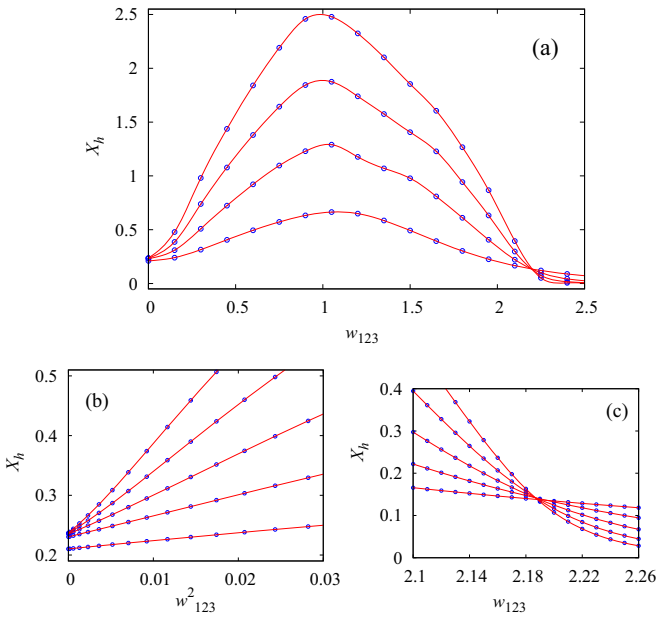

FIG. 5. Finite-size results for the scaled magnetic gaps near the transition to the (1,2,3) phase, versus the rescaled weight w_{123}, in the limit $|J| \to \infty$. (a) The whole range of interest, for system sizes $L =$ 3, 6, 9, and 12. Curves are shown connecting discrete data points. Larger system sizes correspond with steeper curves. More detailed pictures of the data on the left and right parts are shown in (b) and (c) for finite system sizes $L = 3$, 6, 9, 12, and 15.

defined as $X_h(L) \equiv L/[2\pi\xi(K,L)]$, is displayed in Fig. 5 in the vicinity of the transition, versus the rescaled weight w_{123}. The rescaled weights are obtained by dividing out W_{112}, i.e., $w_{123} \equiv W_{123}/W_{112}$, $w_{112} = 1$, and $w_{111} = 0$. The apparent divergence of $X_h(L)$ with L, shown in Fig. 5(a) indicates the existence of an intermediate disordered phase for finite $2|J| + K$. Thus the disordered phase extends all the way to $T = 0$. The behavior on the left-hand side, highlighted in Fig. 5(b), illustrates that the critical state is destroyed by a nonzero w_{123}. Figure 5(b) uses w^2_{123} on the horizontal scale, because (1,2,3) triangles appear in pairs. One thus expects a finite-size dependence according to

$$X_h[w_{123}, L] = X_h + \sum_k p_k w_{123}^{2k} L^{k y_w} + \cdots , \qquad (13)$$

where y_w is the renormalization exponent describing the fugacity of a pair of (1,2,3) triangles. Numerical fits to the transfer-matrix data lead to $y_w \approx 1.4$, with poor apparent convergence. This result seems consistent with $y_w = 3/2$, as expected on the basis of the O(n) magnetic dimension $X_h^{\rm FPL} = 1/2$ reported in Ref. [28] (which is different from the present Potts dimension X_h). The relation with the O(n) dimension follows from the fact that a type (1,2,3) triangle corresponds, along the lines of the mapping described in Sec. III A, with the open end of an O(n) loop segment.

The right-hand side of Fig. 5(a), and the enlarged version in Fig. 5(c), display intersections associated with the transition to the antiferromagnetic phase. Numerical analysis of the intersection points locates this transition near $K - 2J = 0.631$. The data do not permit a clear answer about the type of transition but are suggestive of a weak first-order transition. The amplitude of the correlation length, as determined for finite sizes up to $L = 18$, could not be reliably extrapolated but might seem to correspond with a magnetic dimension of about $X_h = 0.14$.

Thus far we have considered the antiferromagnetic limit $J \to -\infty$, but similar phenomena are also be expected for $J \to +\infty$. For $K \gg -2J$ the (1,2,3) triangles are then excluded, and the mapping on the O(n) model applies. Following the same line of reasoning as for the antiferromagnetic case, one finds from Eq. (9) that an infinite-order transition to the ferromagnetic phase occurs at $K + J = \ln(2)/2$. Finally, the transition to the antiferromagnetic phase takes place close to $K + 2J = 0.631$, mirroring the transition for $J \to -\infty$. The location is verified by Monte Carlo calculations.

IV. CONCLUSION

Our investigation of the phase diagram of the $q = 3$ Potts model on the centered triangular lattice in the (K, J) plane shows the existence of three phases: a ferromagnetic phase dominated by one of the three Potts states, an antiferromagnetic phase where the three different Potts states condense on different triangular sublattices, and an intermediate disordered phase dominated by triangles containing two different Potts states.

In the limits $J \to \pm\infty$, the disordered phase evolves into a state with partial order. There exist, in these limits, infinite ranges of K where the model is critical, and where it is equivalent with the fully packed O(2) loop model on the honeycomb lattice. In addition there are ranges of K at the ferromagnetic sides where the mapping on the O(2) loop model is still valid, but where it is no longer fully packed. The ferromagnetic transitions are of infinite order in these limits. The situation reminds one of the triangular Ising model in a field, which also undergoes a three-state Potts transition, changing into an infinite-order transition when $T \to 0$ [30,36].

On the antiferromagnetic side of the critical ranges, there are ranges of K where the critical state is destroyed by the nonzero weight of triangles with three different Potts spins. While these disordered ranges are, strictly speaking, infinitely wide on the scale of K, they are restricted to $K/|J| = -2$ when $|J| \to \infty$. The transitions between the disordered phase and the antiferromagnetic phase are probably discontinuous for all J.

ACKNOWLEDGMENTS

Z.F. would like to thank C. X. Ding, and W.G. would like to thank F. Y. Wu for valuable discussions. This research was supported by the National Natural Science Foundation of China under Grants No. 11775021, No. 11734002, and No. 11447154, by the Ninth Group of Key Disciplines in Henan Province under Grant No. 2018119, and by the Natural Science Foundation of the Henan Department of Education under Grant No. 18B430012. H.B. acknowledges hospitality extended to him by the Faculty of Physics of the Beijing Normal University.

[1] R. B. Potts, Proc. Camb. Phys. Soc. **48**, 106 (1952).

[2] R. J. Baxter, *Exactly Solved Models in Statistical Mechanics* (Academic Press, London, 1982).

[3] P. Di Francesco, P. Mathieu, and D. Sénéchal, *Conformal Field Theory* (Springer-Verlag, New York, 1997).

[4] F. Y. Wu, Rev. Mod. Phys. **54**, 235 (1982).

[5] J. Adler, A. Brandt, W. Janke, and S. Shmulyian, J. Phys. A **28**, 5117 (1995).

[6] R. Kotecký, J. Salas, and A. D. Sokal, Phys. Rev. Lett. **101**, 030601 (2008).

[7] J. Salas, J. Phys. A **31**, 5969 (1998).

[8] J. K. Burton Jr. and C. L. Henley, J. Phys. A: Math. Gen. **30**, 8385 (1997).

[9] J. Kolafa, J. Phys. A: Math. Gen. **17**, L777 (1984).

[10] M. P. M. den Nijs, M. P. Nightingale, and M. Schick, Phys. Rev. B **26**, 2490 (1982).

[11] J. Salas and A. D. Sokal, J. Stat. Phys. **92**, 729 (1998).

[12] J. P. Lv, Y. Deng, J. L. Jacobsen, and J. Salas, J. Phys. A: Math. Theor. **51**, 365001 (2018).

[13] P. W. Kasteleyn and C. M. Fortuin, J. Phys. Soc. Jpn. **26**(Suppl.), 11 (1969); C. M. Fortuin and P. W. Kasteleyn, Physica (Amsterdam) **57**, 536 (1972).

[14] F. Y. Wu and W. Guo, Phys. Rev. E **86**, 020101(R) (2012).

[15] Y. Huang, K. Chen, Y. Deng, J. L. Jacobsen, R. Kotecký, J. Salas, A. D. Sokal, and J. M. Swart, Phys. Rev. E **87**, 012136 (2013).

[16] R. Kotecký, Phys. Rev. B **31**, 3088 (1985).

[17] Q. N. Chen, M. P. Qin, J. Chen, Z. C. Wei, H. H. Zhao, B. Normand, and T. Xiang, Phys. Rev. Lett. **107**, 165701 (2011).

[18] Y. Deng, Y. Huang, J. L. Jacobsen, J. Salas, and A. D. Sokal, Phys. Rev. Lett. **107**, 150601 (2011).

[19] I. Syozi, in *Phase Transitions and Critical Phenomena*, Vol. 1, edited by C. Domb and M. S. Green (Academic Press, London, 1972), p. 269.

[20] J. L. Cardy, J. Phys. A **17**, L385 (1984).

[21] B. Nienhuis, in *Phase Transitions and Critical Phenomena*, Vol. 11, edited by C. Domb and J. L. Lebowitz (Academic Press, London, 1987), p. 1.

[22] For reviews, see, e.g., M. P. Nightingale, in *Finite-Size Scaling and Numerical Simulation of Statistical Systems*, edited by V. Privman (World Scientific, Singapore, 1990), p. 287; and M. N. Barber, in *Phase Transitions and Critical Phenomena*, Vol. 8, edited by C. Domb and J. L. Lebowitz (Academic, New York, 1983), p. 146.

[23] R. J. Baxter, H. N. V. Temperley and S. E. Ashley, Proc. Roy. Soc. London, Ser. A **358**, 535 (1978).

[24] J. L. Jacobsen and C. R. Scullard, J. Phys. A **46**, 075001 (2013).

[25] J. L. Jacobsen, J. Phys. A **47**, 135001 (2014).

[26] M. X. Wang, J. W. Cai, Z. Y. Xie, Q. N. Chen, H. H. Zhao, and Z. C. Wei, Chin. Phys. Lett. **27**, 076402 (2010).

[27] B. Nienhuis, Phys. Rev. Lett. **49**, 1062 (1982).

[28] H. W. J. Blöte and B. Nienhuis, Phys. Rev. Lett. **72**, 1372 (1994).

[29] J. Kondev and C. L. Henley, Phys. Rev. Lett. **73**, 2786 (1994).

[30] B. Nienhuis, H. J. Hilhorst, and H. W. J. Blöte, J. Phys. A **17**, 3559 (1984).

[31] R. J. Baxter, J. Math. Phys. **11**, 784 (1970).

[32] H. W. J. Blöte, J. L. Cardy, and M. P. Nightingale, Phys. Rev. Lett. **56**, 742 (1986).

[33] I. Affleck, Phys. Rev. Lett. **56**, 746 (1986).

[34] V. L. Berezinskii, Zh. Eksp. Teor. Fiz. **59**, 907 (1970) [Sov. Phys. JETP **32**, 493 (1971)]; J. M. Kosterlitz and D. J. Thouless, J. Phys. C **5**, L124 (1972); **6**, 1181 (1973).

[35] H. W. J. Blöte and M. P. Nightingale, Phys. Rev. B **47**, 15046 (1993).

[36] X. F. Qian, M. Wegewijs, and H. W. J. Blöte, Phys. Rev. E **69**, 036127 (2004).